Diffusion of Triplet Excitons in Crystalline Anthracene

MENAHEM LEVINE AND JOSHUA JORTNER
Department of Chemistry, Tel-Aviv University, Tel-Aviv, Israel
AND
ABRAHAM SZÖKE
Department of Physics, Weizmann Institute of Science, Rehovoth, Israel
(Received 22 March 1966)

In this work we present an experimental study of triplet-exciton diffusion in crystalline anthracene. Triplet-exciton lifetime was determined by the time intermittency method, while the diffusion coefficients and the components of the diffusion tensor were determined by the space intermittency technique. From the comparison of the experimental data with the results of the theoretical analysis we conclude that:

(a) The magnitude of the diffusion coefficient for triplet excitons [$D=(2.0\pm0.5)\times10^{-4}$ cm^2/sec] yields a strong support for the strong scattering random-walk model for triplet-exciton migration in crystalline anthracene.

(b) The diffusion tensor of triplet excitons in crystalline anthracene was found to be isotropic.

(c) The isotropy of the diffusion tensor in the *ab* plane can be properly accounted for in terms of the calculated intermolecular electron exchange and charge-transfer interactions.

I. INTRODUCTION

THE understanding of exciton-transport phenomena in molecular crystals is a subject of considerable current interest. Since an exciton is a mobile nonconducting excited state in a molecular crystal, the experimental and theoretical study of its diffusion process will lead to valuable information regarding the intermolecular electronic interactions and the nature of the scattering mechanism. In spite of recent extensive studies of photoconductivity, exciton spectra, and energy-transfer phenomena, exciton dynamics in molecular crystals is a problem characterized by many subtle complicating effects. These difficulties persist if we limit ourselves to the study of the problems underlying energy-transfer phenomena, which are complicated by exciton trapping, exciton ionization, radiationless decay processes, exciton–exciton annihilation, and other difficulties which exist in the exciton-transport problem. It has not been conclusively demonstrated to date whether the mechanism of energy transfer in molecular crystals involves a coherent motion of the exciton wavepacket, or can be adequately described in terms of an incoherent hopping model.

Recently, some measurements of the diffusion of Wannier excitons in CdS[1] and of Frenkel singlet excitons in crystalline anthracene[2] were performed. Triplet excitons in crystals of aromatic molecules are particularly suitable for experimental study in view of the long lifetime of the triplet state, which is of the order of 10 msec in crystalline naphthalene[3] and anthracene.[4] Indeed, it is now well established that triplet excitons are mobile in molecular organic crystals, and optical emission[5] and electron spin resonance studies[6] of impurity states have been applied for the investigation of triplet energy transfer. The direct population of the first $^3B_{2u}$ state of crystalline anthracene is possible using intense light sources (i.e., lasers[4,7,8] and intense continuous sources[9,10]). Delayed fluorescence on the time scale of milliseconds has been observed in crystalline anthracene.[4,8–10] The delayed fluorescence depends on the square of the light intensity and follows bimolecular kinetics. This effect was interpreted in terms of triplet–triplet annihilation.[4] The collision of two triplet excitons gives rise to a singlet $^1B_{2u}$ exciton state which decays radiatively.

The characteristic long lifetime of triplet excitons in crystalline anthracene enabled Avakian and Merrifield[11] to measure the diffusion constant of triplet excitons. In their experiments a space intermittency method has been applied under conditions of steady illumination. These experiments lead to a diffusion length of $L=10\pm5$ μ, leading to a diffusion coefficient of $D=10^{-4}$

[1] D. G. Thomas and J. J. Hopfield, Phys. Rev. **124,** 654 (1961).
[2] O. Simpson, Proc. Roy. Soc. (London) **A234,** 402 (1956).
[3] P. Avakian (private communication).
[4] R. G. Kepler, J. C. Caris, P. Avkian, and E. Abramson, Phys. Rev. Letters **10,** 400 (1963).
[5] (a) M. A. El-Sayed, M. T. Wauk, and G. W. Robinson, Mol. Phys. **5,** 205 (1962); (b) G. C. Nieman and G. W. Robinson, J. Chem. Phys. **38,** 1928 (1963).
[6] (a) R. W. Bradon, R. E. Gerkin, and C. A. Hutchison Jr., J. Chem. Phys. **37,** 447 (1962); (b) J. Hirota and C. A. Hutchison Jr., *ibid.* **42,** 2869 (1965).
[7] J. L. Hall, D. A. Jennings, and R. M. McClintock, Phys. Rev. Letters **11,** 364 (1963).
[8] S. Singh, W. J. Jones, W. Siebrand, B. P. Stoicheff, and W. G. Schneider, J. Chem. Phys. **42,** 330 (1965).
[9] S. Z. Weisz, B. Zahlan, M. Silver, and R. C. Jarnagin, Phys. Rev. Letters **12,** 71 (1964).
[10] P. Avakian, E. Abramson, R. G. Kepler, and J. C. Caris, J. Chem. Phys. **39,** 1127 (1963).
[11] P. Avakian and R. E. Merrifield, Phys. Rev. Letters **13,** 541 (1964).

TABLE I. Intermolecular interaction matrix elements for the $^3B_{2u}$ state of crystalline anthracene.[a]

Location of molecule	Electron exchange contribution $10^4 K_i$ (eV)	Charge-transfer contribution $10^4 C_i$ (eV)
b	4.10	3.01
$\frac{1}{2}$(**a**+**b**)	−6.83	−2.50
$C+\frac{1}{2}$(**a**+**b**)	0.00	0.42

[a] All other intermolecular interactions are smaller than 10^{-6} eV and can be safely neglected. See Ref. 13.

cm²/sec. In a recent work, Kepler and Switendick[12] studied the effect of crystal thickness on the lifetime of triplet excitons in crystalline anthracene generated by a Q-switched ruby laser. These experiments have demonstrated a marked effect of the crystal thickness on the triplet-exciton lifetime, which was assigned to surface quenching. These experiments lead to a diffusion coefficient of the order 0.4×10^{-2}–2×10^{-2} cm²/sec. A diffusion coefficient of the same order of magnitude was also estimated by Kepler and Switendick[12] from an experimental study of the dependence of the intensity of the delayed fluorescence on the penetration depth of the exciting ultraviolet light in a thick crystal, where triplet excitons are produced by a radiationless transition of singlet excitons. These experimental results are higher by two orders of magnitude from the values previously obtained under the conditions of steady-state illumination.[11] Apart from the numerical discrepancy, the magnitude of the diffusion coefficient makes it possible to distinguish between two different mechanisms for triplet-exciton transfer in crystalline anthracene:

(a) The strong scattering model, characterized by a mean free path of the order of the lattice spacing, wherein the localized states are dominant and the exciton motion can be described in terms of a diffusive, random-walk model.

(b) The coherent-motion band model, where the rate of exciton migration is limited by scattering arising from interaction with the lattice phonons impurities or imperfections and the mean free path is considerably larger than the lattice spacing.

In this work we present an experimental study of triplet-exciton diffusion in crystalline anthracene. The triplet-exciton lifetime, the diffusion coefficients, and the components of the diffusion tensor were measured under conditions of steady illumination. These results make possible a detailed comparison with theoretical data, yielding a strong support for the random-walk model for triplet-exciton migration in molecular crystals or aromatic molecules.

[12] R. G. Kepler and A. C. Switendick, Phys. Rev. Letters **15**, 56 (1965).

II. SURVEY OF THEORETICAL STUDIES OF TRIPLET-EXCITON MIGRATION

A. Interactions

The structure of an exciton band in a molecular crystal is determined by the intermolecular interaction energies. In a detailed study of the triplet-exciton band structure in molecular crystals of aromatic molecules, the following interactions were considered in some detail[13a]:

(a) Intermolecular Coulomb interactions arising from intramolecular spin–orbit coupling between the triplet state of interest and perturbing singlet states. In view of the weak spin–orbit coupling in aromatic hydrocarbons the contribution of the Coulomb integrals to the intermolecular interactions is negligibly small.

(b) Intermolecular electron exchange interactions which can be displayed in the form:

$$K^f_{n1,m\mu}=\langle(\mathfrak{A}-1)\varphi_{n1}{}^f\varphi_{m\mu}{}^0 \mid V_{n1,m\mu} \mid \varphi_{n1}{}^0\varphi_{m\mu}{}^f\rangle, \quad (1)$$

where $\varphi_{kl}{}^i$ is the electronic wavefunction in the k, lth lattice site and in the ith electronic state, $V_{n1,m\mu}$ is the intermolecular interaction potential, while $\mathfrak{A}$ represents the intermolecular antisymmetrization operator. These electron-exchange interactions lead to the major contribution to the intermolecular interactions and to the Davydov splitting in the triplet state of aromatic crystals. A detailed analysis has shown[13a] that non-orthogonality corrections are small and the effects of crystal-field mixing between different triplet states are negligible. The intermolecular electron exchange integrals for the anthracene crystal previously calculated using antisymmetrized products of Hückel orbitals[13b] are presented in Table I. These interactions lead to a total electronic contribution of 43 cm^{-1} for the Davydov splitting in the first exciton state of the anthracene crystal, and 45 cm^{-1} for the splitting in the first triplet-exciton state of crystalline naphthalene. Within the framework of the weak vibronic coupling scheme, which is obviously appropriate for this case,[13a] the contribution of the electron exchange interactions to the splitting in the 0–0 vibronic band of the $^3B_{2u}$ state of anthracene and naphthalene is 9 cm^{-1}.

(c) An additional contribution to the intermolecular interactions in the triplet state arises from configuration interaction with ion-pair exciton states.[14] These ion-pair states, though not detected experimentally, are presumably located at about 1.5–2 eV above the first

[13] (a) J. Jortner, S. A. Rice, J. L. Katz, and S. I. Choi, J. Chem. Phys. **42**, 309 (1965). (b) A slight numerical error was discovered in the intermolecular electron exchange matrix elements presented by Jortner, Rice, Katz, and Choi in Ref. 13(a). The corrected data have been recently reported by Rice and Jortner [S. A. Rice and J. Jortner, *Physics of Solids at High Pressures*, C. T. Tonuzuka and R. M. Emrich, Eds. (Academic Press Inc., New York, 1965), p. 63].

[14] S. I. Choi, J. Jortner, S. A. Rice, and R. Silbey, J. Chem. Phys. **41**, 3294 (1964).

triplet state in crystalline anthracene and naphthalene. The mixing between the neutral and charge-transfer states was considered in detail by Choi *et al.*[14] The contribution of the ion-pair states is expected to increase the intermolecular interactions in the triplet state by about 30%–50%. These contributions of the charge transfer are summarized in Table I.

The theoretical estimates of the total electronic contribution to the Davydov splitting in the $^3B_{2u}$ state of simple aromatic crystals can now be readily obtained. For the case of crystalline naphthalene we get 65 cm^{-1} (consisting of 45 cm^{-1} from the electron exchange and 20 cm^{-1} from the charge-transfer contributions), while for the case of crystalline anthracene, the estimated Davydov splitting is 59 cm^{-1} (43 cm^{-1} from electron exchange and 16 cm^{-1} from charge-transfer interactions). As it was often stressed,[13a,14] these theoretical estimates are reliable only within a numerical factor of about 2–3. A striking experimental confirmation of these theoretical estimates has recently been provided by Robinson and Hanson[15] who studied the Davydov splitting in the first triplet state of crystalline naphthalene. The total splitting of 38 cm^{-1} in all the vibronic components was obtained while the splitting in the 0–0 vibronic band was found to be 12 cm^{-1}, in excellent agreement with the theoretical predictions. We thus conclude that in the first excited triplet state of some typical aromatic crystals (i.e., naphthalene and anthracene), the intermolecular pair interactions between adjacent molecules are of the order of 5 cm^{-1}.

B. Hopping Model for Triplet-Exciton Migration

Triplet-exciton migration in organic crystals is determined by relatively small intermolecular interactions. As these interactions are much smaller than the intramolecular vibration energies, the weak vibronic coupling scheme should be applicable for this case. For a given triplet crystal state we should consider a set of vibronic sublevels separated by the intramolecular vibrational quantum (which is of the order of 1000 cm^{-1}). This coupling can be considered as a static effect, modifying the electronic interaction matrix elements by multiplying them by a Franck–Condon vibrational overlap factor. Exciton scattering occurs by interaction with the intermolecular vibrations and, in particular, with acoustic modes. The off-diagonal matrix elements of the crystal Hamiltonian are small even compared with the frequency of the intermolecular lattice vibrations. Under these conditions the rate of triplet-excitation transfer will be small compared with the lattice relaxation time. The coupling of the exciton state with the lattice phonons is expected to be strong enough to cause elastic scattering at every lattice site, and thus to destroy the crystal momentum as a good quantum number. Under these extreme conditions of strong scattering of the exciton wave, the mean free path is of the order of magnitude of the intermolecular separation in the crystal and the motion of the excitation can be described as a random walk, i.e., a diffusion process. The small but finite off-diagonal matrix elements result in a random hopping from one localized state to another. We thus consider resonance transfer of the triplet excitation between localized states. The resonance-transfer probability is a sensitive function of the vibrational state of the lattice, in view of the exponential dependence of the transfer integrals on the intermolecular spacing. A detailed theory of acoustic mode scattering within the framework of the tight binding approximation has to include these effects.[16] For the study of the random-walk model we limit ourselves to a discrete probability distribution based on the intermolecular interaction integrals at the equilibrium configuration of the crystal. These intermolecular interaction integrals have to be related to the probability of exciton transfer. Application of first-order time-dependent perturbation theory leads to conventional expression for the transition probability $W(1\,\alpha \mid i\beta)$ for energy transfer from the reference molecule 1 in the vibrational state α to Molecule i in the vibrational state β,

$$W(1\,\alpha \mid i\beta) = (2\pi/\hbar) \mid J(1\,\alpha \mid i\beta) \mid^2 \rho(E_f), \quad (2)$$

where $J(1\,\alpha \mid i\beta)$ is the transfer integral and $\rho(E_f)$ is the density of final states. The transfer integrals are related to the electronic interaction matrix elements by the simple expression

$$J(1\,\alpha \mid i\beta) = (K_{1i}+C_{1i})\,\langle \chi^{f(\beta)} \mid \chi^{0(\alpha)} \rangle^2, \quad (3)$$

where K_{1i} and C_{1i} are the electronic contributions to electron exchange and charge-transfer interactions and $\langle \chi^{f(\beta)} \mid \psi^{0(\alpha)} \rangle$ represents the intramolecular vibrational overlap integral between the αth and βth vibrational states corresponding to the ground and the fth electronic excited state, respectively.

The Franck–Condon overlap integrals can be estimated from the relative intensities of the vibronic components in the phosphorescence spectrum of the aromatic molecule in a rigid glass, or estimated theoretically.[13a] A typical value for the Franck–Condon factor suitable for approximate numerical calculation is $\langle \chi^{f(\beta)} \mid \chi^{0(\alpha)} \rangle^2 = 0.25$. Note that energy-conservation rules imply that $\alpha = \beta$. The spectral weight function representing the local density of states is approximated by assuming a uniform distribution of states through the exciton band, characterized by a total width ΔE so that $\rho(E_f) = 1/\Delta E$. Using these approximations the mean lifetime τ_e of an excitation on the reference molecule is given by

$$1/\tau_e = \sum_i W(1\,\alpha \mid i\alpha) \quad (4)$$

[15] D. M. Hanson and G. W. Robinson, J. Chem. Phys. **43,** 4174 (1965).

[16] L. Friedman, Phys. Rev. **140,** A1649 (1965).

TABLE II. Electron exchange contribution to triplet-exciton bandwidth in crystalline anthracene.

Direction of k vector	Energy units (10^{-4}eV)
$(a^{-1})_+$	27.36
$(a^{-1})_-$	27.36
$(b^{-1})_+$	11.41
$(b^{-1})_-$	43.76
$(c^{-1})_+$	0.09
$(c^{-1})_-$	0.08

and the components of the diffusion tensor D are given by

$$D_{\mu\nu}=\sum_i(\pi/\hbar\Delta E)\mid J(1\,\alpha\mid i\alpha)\mid^2(\mathbf{r}_1-\mathbf{r}_i)_\mu(\mathbf{r}_1-\mathbf{r}_i)_\nu. \tag{5}$$

The application of first-order perturbation theory might appear questionable, as the effects of intermediate virtual states have been neglected, and as the final density of states is not well defined within the framework of the localized model. Nevertheless, it is the opinion of the authors that Eq. (5) can be used with some confidence as an analogous result can be derived for a very similar case, that of excess electron mobility in aromatic solids, on the basis of Kubo's formalism[17] of the linear response theory.[18] In the general expression derived herein for the mobility tensor, the individual jump frequencies are calculated from the contributions of molecular pair interactions. Each jump frequency is weighted according to the quadratic displacement vectors. Even in this approximation, considerable difficulty remains in estimating the bandwidth and the density of states. Two relatively simple formulas suggest themselves for this purpose.

The first approach involves neglecting the charge-transfer interactions. In this case, ΔE represents the total exciton bandwidth $\Delta\mathcal{E}$ calculated using the contribution of electron exchange interactions only, modified by the vibrational overlap factor. The numerical values for the total electronic contribution to the triplet-exciton bandwidths in crystalline anthracene parallel to the reciprocal lattice vectors is presented in Table II. In this case of a monoclinic crystal (symmetry C_{2h}^5) two energy bands arise in the first Brillouin zone involving symmetric (+) and antisymmetric (−) combinations of molecular wavefunctions corresponding to two molecules per unit cell. In this case, the components of the diffusion tensor can be displayed in the form

$$D_{\mu\nu}=\sum_i(\pi/\hbar\Delta\mathcal{E})K_{1i}^2\langle\chi^{0(\alpha)}\mid\chi^{f(\alpha)}\rangle^2X_{1i}^{\mu}X_{1i}^{\nu}, \tag{6}$$

where X_{1i}^{μ} is the component of the vector $\mathbf{r}_1-\mathbf{r}_i$ along the μth crystal axis. In this approximation when electron exchange interactions only are included, the energy of the exciton state depends very little on the **c** component of the **k** vector. The band structure is similar to the band structure of a two-dimensional crystal formed by the *ab* plane. We take a total bandwidth to represent a constant density of states throughout the whole band. From the data of Table II, we set $\Delta\mathcal{E}=55$ cm^{-1}. The calculated data for the triplet-exciton diffusion tensor in crystalline anthracene are presented in Table III.

When charge-transfer interactions are included in the formalism, we can assume that the energy denominator determining the density of states is represented by the sum of the intermolecular interactions

$$\Delta E=\langle\chi^{0(\alpha)}\mid\chi^{f(\alpha)}\rangle^2\sum_i(K_{1i}+C_{1i}), \tag{7}$$

leading to the result

$$D_{\mu\nu}=(\pi/\hbar)\langle\chi^{0(\alpha)}\mid\chi^{f(\alpha)}\rangle^2\times[\sum_i(K_{1i}+C_{1i})^2X_{1i}^{\mu}X_{1i}^{\nu}/\sum_i(K_{1i}+C_{1i})]. \tag{8}$$

This result is similar to that recently obtained by Glaeser and Barry[19] using a hopping model involving incoherent jumps and relating the quadratic moments of probability distribution for the radial displacements to the quadratic moments of the jump probabilities using Chandrasekhar's scheme.[20] This treatment was applied to the study of electron and hole mobilities[19] and to the investigation of triplet-exciton diffusion in organic crystals.[21] The results of the calculations of the components of the diffusion tensor in crystalline anthracene are displayed in Table III. The off-diagonal components were found to be negligible. From these results we conclude that:

(a) The theoretical value for the mean diffusion coefficient $D\approx\frac{1}{3}(D_{aa}+D_{bb}+D_{cc})$ is 4×10^{-4} cm^2/sec calculated including electron exchange interactions only.

(b) The inclusion of charge-transfer interactions increases the absolute value of the components of the diffusion tensor by a numerical factor of about 2.

(c) The components of the diffusion tensor in the

TABLE III. Theoretical calculations of the components of the diffusion tensor for triplet excitons in crystalline anthracene for the hopping model.

	$10^4\,D_{ii}$ (cm^2/sec)	
	Electron exchange contribution [Eq. (6)]	Electron exchange and charge-transfer contribution [Eq. (7)]
D_{aa}	5.88	13.33
D_{bb}	5.50	15.64
D_{cc}	0.00	0.12

[17] R. Kubo, J. Phys. Soc. Japan **12**, 570 (1957).

[18] P. Goar and S.-I. Choi, "Theory of Electron and Hole Mobility in Aromatic Solids," J. Chem. Phys. (to be published).

[19] R. M. Glaeser and R. S. Berry, J. Chem. Phys. **44**, 3797 (1966).

[20] S. Chandrasekhar, Rev. Mod. Phys. **15**, 1 (1943).

[21] R. S. Berry (private communication).

ab plane are expected to be about equal, i.e., $D_{aa}/D_{bb}=1.06$. The inclusion of the charge-transfer states does not markedly affect the anisotropy of the diffusion tensor in the ab plane.

(d) The inclusion of charge-transfer states alters the model of triplet-exciton migration in one aspect[13a]: when electron exchange interactions only are considered, the triplet-exciton motion is restricted to the ab plane, while mixing of charge-transfer states leads to a sizable interaction with the molecule located at $\mathbf{c}+\frac{1}{2}(\mathbf{a}+\mathbf{b})$ and the motion of the triplet exciton is not confined to the ab plane.

C. Band Model

The band structure calculations[13a] can be applied to estimate the diffusion coefficient of triplet excitons within the framework of the band model. Adopting the conventional phenomenological approach, we assume that the exciton scattering can be described in the constant relaxation time approximation the components of the diffusion tensor can be expressed in the form

$$D_{\mu\nu}=\tau_s\langle V_\mu V_\nu\rangle \tag{9}$$

or

$$D_{\mu\nu}=\Lambda\langle V_\mu V_\nu/|\,\mathbf{V}(\mathbf{k})\,|\rangle, \tag{10}$$

where V_μ and V_ν are the components of the group velocity $\mathbf{V}(\mathbf{k})$,

$$\mathbf{V}(\mathbf{k})=(1/\hbar)\nabla_{\mathbf{k}}E(\mathbf{k}). \tag{11}$$

τ_s is a constant isotropic relaxation time, while Λ is an isotropic mean free path, i.e., $\Lambda=\tau_s\langle|\,\mathbf{V}(\mathbf{k})\,|\rangle$. The angular brackets represent the average over the Boltzmann distribution of excitons in the band. While it is not possible to calculate the absolute value of the diffusion coefficient in the band scheme, it is possible to estimate the anisotropy of the diffusion tensor. The theoretical results for the velocity components using electron exchange interactions only are displayed in Table IV. The predicted anisotropy of the diffusion tensor in the ab plane is $D_{aa}/D_{bb}=1.15$.

It is interesting to note that in the limiting case of strong scattering, the numerical results derived from the band model and from the hopping model are comparable. Setting $\Lambda=5$ Å, which is of the order of intermolecular separation, we get for the band model $D_{aa}=3.6\times10^{-4}$ cm^2/sec and $D_{bb}=3.1\times10^{-4}$ cm^2/sec, which are comparable with the results previously derived for the random-walk model.

TABLE IV. Velocity components for triplet excitons in crystalline anthracene calculated using electron exchange interactions only.

μ	ν	$\langle v_\mu v_\nu/\|\mathbf{v}(\mathbf{k})\|\rangle$ (10^4 cm/sec)	$\langle v_\mu v_\nu\rangle$ (10^9 cm^2/sec^2)
a	a	0.605	0.801
b	b	0.520	0.694
c	c	0.00	0.00

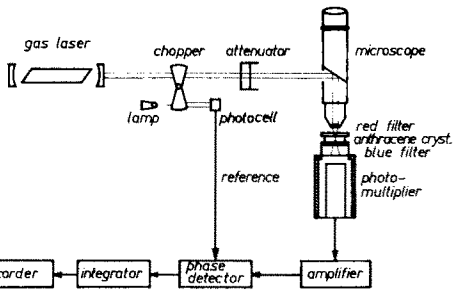

FIG. 1. Schematic diagram of the experimental arrangements.

III. EXPERIMENTAL METHODS

Triplet excitons were generated by direct absorption of light from a red helium–neon gas laser ($\lambda=6328$ Å). The laser output was 1.5 mW at a multimode operation. Light of such wavelength penetrates the crystal practically unattenuated, the absorption coefficient being $\alpha=3\times10^{-4}$ cm^{-1}.

The experimental arrangement is shown in Fig. 1. The incoming light was attenuated by a variable-length absorption cell containing copper sulfate, passed through the illumination mechanism of a metallurgical microscope, and focused on the crystal. The crystal plane was oriented perpendicular to the incident laser beam. The light was focused to form a circular area of radius R_0 in the ab plane, R_0 was varied in the region 8–150 μ. In another set of experiments, the light was focused by a cylindrical lens so that the crystal was illuminated in a narrow slab of width $D_0=10$–20 μ and thickness of 500 μ. In all cases, the electric vector of the incident light was maintained parallel to the crystal axes to eliminate spurious effects arising from double refraction. The distribution of the incident light was determined photographically (Fig. 2) demonstrating that the incident beam remains in form of a narrow beam upon transversing the crystal. The size of the illuminated spot could be varied by changing the divergence of the

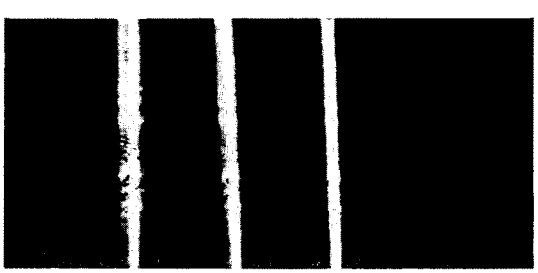

FIG. 2. The distribution of the incident light within the crystal. The photographs show the intensity distribution for a slab, with the laser light passed through the optical system, and emerging through a 0.3-mm-thick anthracene crystal. The thickness of the slab (from left to right): $D_0=24$ μ, $D_0=24$ μ, $D_0=34$ μ, and $D_0=48$ μ.

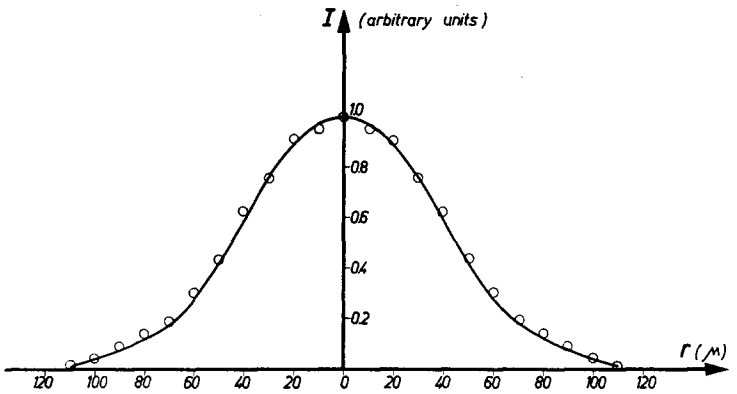

FIG. 3. The radial distribution of the incident intensity for a radial spot of $R_0=110\ \mu$. The laser was operated at a single mode. The solid curve is calculated according to Eq. (15).

beam as it entered the microscope or by changing the height of the microscope stage. The intensity distribution in the irradiated area was measured using a 10-μ hole and a calibrated microscope state (Fig. 3). It was found to be in agreement with calculations using the optical properties of the illumination system. Two Corning filters cut out any blue background light which could excite singlet excitons directly. Below the crystal there were two Corning glass filters to cut out light of wavelength longer than 7000 Å and a cell of methylene blue which has the measured attentuation of 10^{-16} for the wavelength of the laser. The "blue" light was collected by an EMI 6256 photomultiplier, and finally registered on a recorder after electronic integration. The electronic system consisted of a dc current amplifier (Keithley 417), a synchronous mechanical chopper using mechanical relays (operated at 2 cps), and an electronic integrator (converted Keithley 610). The voltage at the chopper was kept at the order of 1 V. This corresponded to an input current of 3×10^{-10} A at the highest gain which was actually used. At lowest light levels, this consisted mostly of the dark current of the photomultiplier. The longest integration times used were 5 min, and the integrator had a 2% stability over an hour. The lowest integration rates corresponded to a flux of 2×10^3 photon/sec on the photocathode. All the experiments were performed at room temperature ($T=300$°K).

Single crystals of anthracene cleaved along the *ab* or the *ac* plane were cut from melt-grown ignots. The latter were prepared from commercial anthracene by repeated zone refining.

IV. KINETIC CONSIDERATIONS

Under the conditions of steady illumination the concentration ρ of triplet excitons is determined by the equation

$$(\partial\rho/\partial t)+\mathrm{div}\,\mathbf{j}=-\beta\rho-\gamma\rho^2+S(\mathbf{r}), \qquad (12)$$

where $\mathbf{j}$, the particle (i.e., exciton) current density, is related to the diffusion tensor D by

$$j_\mu=\sum_\nu D_{\mu\nu}(\partial\rho/\partial X_\nu); \qquad (13)$$

β^{-1} is the lifetime of the triplet exciton and γ the bimolecular recombination rate constant. The available kinetic data are summarized in Table V. $S(\mathbf{r})$ represents the source function for the creation of triplet excitons by the laser light. For the experimental conditions employed in this work, steady-state conditions apply, so that $\partial\rho/\partial t=0$.

We briefly consider the simple case of a uniform flux of exciting light (the size of the irradiated area is large relative to the exciton diffusion length). Equation (12) reduces then to the conventional form

$$\alpha I-\beta\rho-\gamma\rho^2=0, \qquad (14)$$

where α is the absorption coefficient and I the incident-light intensity. The intensity of the blue emission F, due to triplet–triplet annihilation, is $F=\frac{1}{2}\gamma\rho^2$. At low intensities (i.e., $\beta\rho\gg\gamma\rho^2$), $\rho=\alpha I/\beta$, and $F=(\alpha\gamma^2/2\beta^2)I^2$, while at high intensity (i.e., $\beta\gg\gamma\rho$), $\rho=(\alpha I/\gamma)^{\frac{1}{2}}$ and $F=\frac{1}{2}\alpha I$. In Fig. 4 we display the dependence of the intensity blue fluorescence on the exciting red light intensity. At low exciting intensities the emitted blue fluorescence depends on I^2, while the deviation at high intensities represents the transition to the linear region Under steady-state conditions, the contribution of fluorescence generated by two-photon absorption is negligible. In this case, double-photon excitation, the blue fluorescence P depends on the square of the flux $P=KI^2$. The best value of K for anthracene is that of

TABLE V. Experimental kinetic data for triplet excitons in crystalline anthracene.

α (cm^{-1})	β (sec^{-1})	γ (cm^3 sec^{-1})
2.1×10^{-5} ($\lambda=6943$ Å)[a]	100[a]	2.5×10^{-11}[a]
		4×10^{-11}[b]
3.4×10^{-4} ($\lambda=6200$ Å)[b]	57–440[c]	
	100–200[d]	$(2.8\text{–}6.7)\times10^{-11}$[c]

[a] Reference 4.
[b] Reference 10.
[c] Reference 8.
[d] Present work.

Hall *et al.*,[7] $K=1.26\times10^{-29}$ cm·sec photon^{-1} at 6943 Å. Hence at low light intensities and steady illumination, the ratio of the blue fluorescence due to exciton annihilation and that arising from double-photon absorption is $F/P=\gamma\alpha^2/2\beta^2K$, independent of the light intensity. This ratio is about $F/P=10^{+6}$ and the double-photon excitation process is negligible under the experimental conditions employed herein.

All the exciton-diffusion experiments were performed at sufficiently low intensities, where the triplet-exciton concentration is proportional to the exciting light intensity, so that the bimolecular annihilation channel does not affect the triplet-exciton concentration but is merely used as a monitoring device for the determination of the local exciton concentration.

Diffusion coefficients were determined by the space intermittency method. The crystal is illuminated by a narrow pattern of light, and the total intensity F of the emitted blue fluorescence is recorded as a function of the size of the irradiated area S at a constant intensity of the exciting light. Since the intensity of the blue fluorescence depends on the square of the exciton concentration it will depend on the spatial distribution of triplet excitons, which is affected by the exciton-diffusion process. When the dimensions of the irradiated area are small relative to the diffusion length of the triplet exciton a substantial fraction of the triplets will diffuse out of the illuminated region and the spatial exciton distribution and hence the integrated intensity F will be independent of s. On the other hand, when the dimensions of the irradiated area are large relative to the diffusion length, F will be inversely proportional to s. It should be emphasized that even if the recombination rate is strongly direction dependent, i.e., the recombination rate constant γ is anisotropic, it is only the diffusion rate in the direction of the smallest dimension of the illuminated spot which is measured. The quantitative description of the effect of exciton-diffusion process on F is obtained from the solution of the diffusion equation (12) under steady-state conditions followed by the evaluation of the integral $F=(\gamma/2)\int\rho^2dv$, where v is the total volume of the crystal.

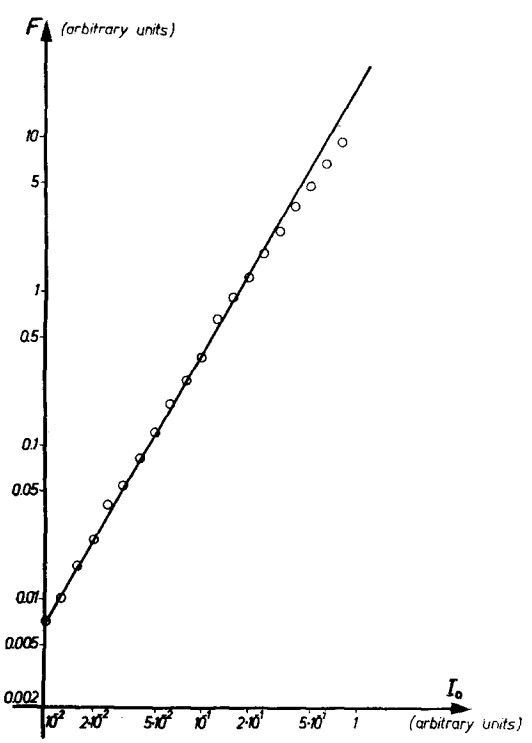

FIG. 4. The dependence of the intensity of the blue fluorescence on the total intensity of the laser. A radial spot with $R_0=50$ μ was irradiated with the laser operated multimode. The solid line shows the dependence $F\propto I_0^2$.

The differential equation (12) cannot be solved in a closed form. Relatively simple iterative solutions can be obtained if we restrict ourselves to an isotropic diffusion coefficient and to some simple geometrical distribution of the exciting light. The analytical solutions of the diffusion equation are discussed in the Appendix. The determination of the mean diffusion coefficient in the *ab* crystal plane was performed by illuminating a circular area (of radius R_0), with the crystal *ab* plane oriented perpendicular to the incident beam. The intensity distribution in the *ab* plane was experimentally monitored by a slit of 10-μ thickness. The source function was experimentally found to be

$$S(r)=G\left[\frac{\sin(\pi r/R_0)}{(\pi r/R_0)}\right]^2, \qquad r<R_0,$$
$$S(r)=0, \qquad r>R_0, \tag{15}$$

where G is a constant corresponding to $S(0)$. Results representing typical experimental data are presented in Fig. 3. These data are consistent with the classical formula for diffraction by a slit. The solutions of the diffusion equation

$$D\left[r^{-1}\frac{\partial}{\partial r}\left(r\frac{\partial\rho}{\partial r}\right)+\frac{1}{r^2}\frac{\partial^2\rho}{\partial\phi^2}+\frac{\partial^2\rho}{\partial Z^2}\right]-\beta\rho-\gamma\rho^2+S(\mathbf{r})=0 \tag{16}$$

were determined by numerical integration for $\gamma=4\times10^{-11}$ cm^3 sec^{-1}, $\beta=100$–200 sec^{-1}, $S(\mathbf{r})$ given by Eq. (15), R_0 varying in the range 0–200 μ for various values of the (isotropic) diffusion coefficient. The numerical integration of the differential equation was performed using a 1604 CDC computer at the Weizmann Institute of Science.

The components of the diffusion tensor were determined by illuminating the crystal in a slab (Fig. 2) whose small dimension was perpendicular to the *ab* plane or to the *ac* plane. The crystal was oriented so that the narrow band was parallel to one of the crystal axes, permitting the determination of the diffusion coefficient along the axis perpendicular to it.

Under the ideal conditions of uniform flux, $S=\alpha I$ for $X<d$ and $S=0$ for $X>d$, the diffusion equation

for the slab is

$$\alpha I-\beta\rho+D(\partial^2\rho/\partial X^2)=0. \quad (17)$$

When the light slab is perpendicular to the ith crystal axis, the spatial distribution of exciton is determined by the D_{ii} component of the diffusion tensor. The solution of the diffusion equation (17) is

$$\rho=(\alpha I/\beta)[1-\exp(-\omega_i d/2)\cosh(\omega_i X)], \quad -\tfrac{1}{2}d\leq X\leq\tfrac{1}{2}d,$$

$$\rho=(\alpha I/\beta)\sinh(\omega_i d/2)\exp(-\omega_i X), \quad \tfrac{1}{2}d\leq X\leq-\tfrac{1}{2}d, \quad (18)$$

where

$$\omega_i=(\beta/D_{ii})^{\frac{1}{2}}. \quad (19)$$

The diffusion length is given by $l_i=\sqrt{2}/\omega_i$. The total blue photon flux is now given by

$$F=(\gamma\alpha^2I^2L/2\beta^2)\times\{d-(3/2\omega_i)+\exp(-\omega_i d)[(3/2\omega_i)+\tfrac{1}{2}d]\}, \quad (20)$$

where L is the length of the slab.

The photon flux I can be related to the total light intensity incident on the crystal I_0 by $I=I_0/Ld$, and Eq. (20a) takes the form

$$Fd=C\{1-(3/2\omega_i)+\exp(-\omega_i d)[(2/3\omega_i d)+\tfrac{1}{2}]\}, \quad (20')$$

with $C=\gamma\alpha^2I_0^2/2\beta^2L$. The distribution of the incident light intensity is not uniform, but given by Eq. (15). Machine calculations have shown that the total blue photon flux can be represented by Eq. (20) with $d=D_0/2$, where D_0 is the total width of the illuminated area.

From the kinetic analysis presented herein, we conclude that:

(a) At low light intensities, F is determined by the square of the total light intensity, even when the spatial distribution of excitons is determined by diffusion.

(b) The dependence of F on α^2 makes possible an experimental determination of the polarization of the singlet–triplet transition.

(c) Although the bimolecular triplet–triplet annihilation rate constant may be anisotropic, the experimental situation does not enable us the determination of this anisotropy as F depends on the space integral of ρ^2, introducing an average value for γ.

V. LIFETIME OF TRIPLET EXCITONS IN CRYSTALLINE ANTHRACENE

In view of the discrepancy obtained between the diffusion length observed under steady-state illumination[11] and the diffusion coefficient observed under transient conditions,[12] the possibility arises that the steady-state illumination technique is fraught with difficulties in view of exciton-trapping effects, which may change the exciton lifetime and affect the diffusion length. It was therefore considered important to gain experimental information regarding triplet lifetimes under quasi-steady-state illumination.

Triplet-exciton lifetimes were determined by the time intermittence method. Intermittent illumination of the crystal was performed by a rotating-sector disk, the duration of the illumination and light cutoff times being equal. The integrated emitted intensity was measured as a function of the irradiation time τ. The effect of intermittent illumination can be qualitatively interpreted by the following considerations: If a number of excitons are generated during the irradiation, then cessation of the illumination, the exciton concentration is reduced to zero, the decay being determined by the exciton lifetime. When the light is switched on, the cycle of events is repeated. On the other hand, if the second period of illumination occurs before the exciton concentration has fallen to zero, then the second crop of excitons interferes with the concentration of the first lot. Since the intensity of the delayed fluorescence varies as the square of the exciton concentration, we expect that the integrated intensity of the fluorescent light will vary fairly rapidly with the speed of the rotation of the sector when the lifetime between flashes is of the order of the exciton lifetime. Below and above this value, the intensity is independent of the illumination period. The sector was cut so that the periods of light and dark are equal in duration, the ratio of other maximum and minimum intensities is then expected to be 2:1. Under conditions of relatively low exciton concentration ($\beta\gg\gamma\rho$) generated in an illuminated area which is large relative to the diffusion length, the situation is described by the simple kinetic equations

$$d\rho/dt=\alpha I-\beta\rho, \quad 0\leq t\leq\tau,$$
$$d\rho/dt=-\beta\rho, \quad \tau\leq t\leq 2\tau. \quad (21)$$

The solutions of Eq. (21) are given by

$$\rho(t)=(\alpha I/\beta)(1-\{\exp(-\beta t)/[1+\exp(-\beta\tau)]\}), \quad 0\leq t\leq\tau,$$

$$\rho(t)=(\alpha I/\beta)(\{\exp[-\beta(t-\tau)]/[1+\exp(-\beta\tau)]\}), \quad \tau\leq t\leq 2\tau. \quad (22)$$

The total blue photon flux F emitted from the crystal is then proportional to the integral $\int\rho^2(t)dt$. It is convenient to express the final result in the form

$$F/F_\infty=1-[\tanh(\tfrac{1}{2}\beta\tau)/\beta\tau], \quad (23)$$

where F_∞ is the limiting value of F for $\tau\to\infty$ (i.e., $\tau\gg\beta^{-1}$). F_∞ is just $F_\infty=0.5\,F_s$, where F_s is the intensity of the blue light obtained under conditions of steady illumination without chopping.

The plots of Eq. (23) are presented in Fig. 5 where

we have displayed the experimental data obtained for several crystals of anthracene. In these experiments, the illuminated area was a circular spot with $R_0=200\ \mu$. The experimental values of β obtained under conditions of quasicontinuous illumination are displayed in Tables V and VII. From the results, we conclude that the values of β obtained from quasi-steady-state illumination are identical with those previously reported from transient measurements. It thus appears that trapping effects do not contribute to the triplet-exciton lifetime, and the monomolecular decay involves free excitons. We thus infer that the crystals used are pure enough so that the excitons are free to move through the crystal either by a coherent motion via the triplet band or by a random-walk motion. This conclusion is consistent with the lack of variation of β with temperature as reported by Singh *et al.*[8] The variation of the β values in different crystals is of the order of 50%, and the highest value of the lifetime obtained herein is $\beta^{-1}=10$ msec. On the basis of these experiments, it cannot be established whether this is the intrinsic lifetime of triplet excitons in the crystal, or it is due to an enhanced radiationless transition involving collision of triplet excitons with impurities. It was recently pointed out that the intrinsic lifetime of triplet excitons in pure aromatic crystals can be short as an efficient channel for vibrational relaxation in the crystal is available.[22] The lack of phosphorescence[5b] in pure crystals of benzene, naphthalene, and anthracene should be attributed to the decrease of the lifetime of the triplet state arising from an efficient monomolecular decay process.[22]

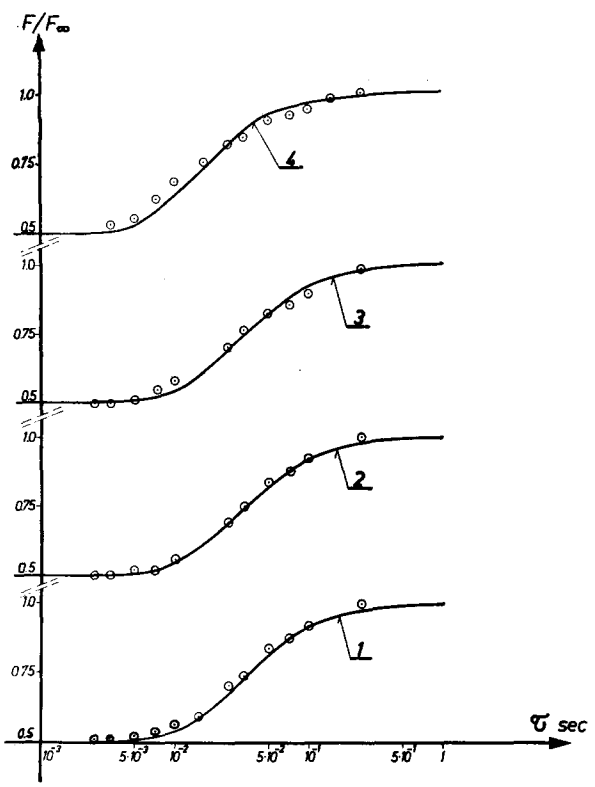

FIG. 5. The experimental determination of triplet-exciton lifetime in crystalline anthracene by the time intermitting method. The experimental points represent the dependence of the integrated intensity of blue fluorescence on the irradiation period. The solid curves are calculated from Eq. (23): (1) 0.3-mm zone-refined crystal irradiated perpendicular to the *ab* plane, $\beta=113$ sec^{-1}; (2) 0.3-mm zone-refined crystal irradiated perpendicular to the *ab* plane, $\beta=115$ sec^{-1}; (3) 0.4-mm zone-refined crystal irradiated perpendicular to the *ac* plane, $\beta=125$ sec^{-1}; (4) 0.5-mm zone-refined crystal irradiated perpendicular to the *ab* plane, $\beta=200$ sec^{-1}.

VI. POLARIZATION RATIOS FOR THE SINGLET–TRIPLET TRANSITION

The use of the polarized laser source makes possible an accurate experimental determination of the polarization ratios for the ${}^1A_{1g}\rightarrow{}^3B_{2u}$ transition in crystalline anthracene. When the dominant channel for triplet-exciton decay involves the unimolecular process, analytical and numerical solutions of the diffusion equation show that F depends on α^2. The polarization of the singlet–triplet transition was determined by irradiation of the crystal at constant intensity, with the light polarized parallel to the crystal axes, followed by the subsequent determination of the intensity of the blue fluorescence. Polarization ratios were determined with the beam incident to the *ab* or to the *ac* crystal planes. The experimental data are displayed in Table VI. These results are consistent with the data previously reported by Avakian *et al.*[10] The polarization ratios for transition polarized along the long molecular axis (L), short molecular axis (M), and the axis perpendicular to the molecular plane (N) can be evaluated within the framework of the oriented gas model using the known crystal structure[23] (Table VI). The oriented gas model appears to be adequate for the treatment of triplet states of aromatic solids, as the contribution of crystal field mixing between triplet exciton states is negligible[13a] and the off-diagonal matrix elements combining the states are negligible in comparison with the energy separation between these triplet states.

The experimental results for the polarization ratios indicate that a significant component of the transition moment arises from spin–orbit coupling with singlet excitations polarized perpendicular to the molecular plane. As it is well known, spin–orbit coupling in aromatic hydrocarbons is extremely weak.[24] McClure[24a] has shown that when spin–orbit coupling between $\pi\rightarrow\pi^*$ excitations is considered, leading to an in-plane component of the transition moment for the singlet–triplet transitions, only three-center contributions have to be included. Spin–orbit coupling between triplet $\pi\rightarrow\pi^*$

[22] H. Y. Sun, J. Jortner, and S. A. Rice, J. Chem. Phys. **44**, 2539 (1966).
[23] R. Silbey, J. Jortner, and S. A. Rice, J. Chem. Phys. **42**, 1515 (1965).
[24] (a) D. S. McClure, J. Chem. Phys. **20**, 682 (1952); (b) M. Mizushima and S. Koide, *ibid.* **20**, 765 (1952).

TABLE VI. Polarization rates for the $^1A_{1g} \rightarrow {}^3B_{2u}$ transition in crystalline anthracene.

Crystal plane	Polarization ratios	Experimental polarization ratios		Calculated polarization ratios		
		Present work	Ref. 10	Transition L polarized	Transition M polarized	Transition N polarized
ab	$P(a/b)$	2.35±0.1	1.4	15.8	0.13	3.4
ac	$P(a/c)$	2.0±0.2	1.6	0.33	1.05	4.0

states and singlet $\sigma \rightarrow \pi^*$ (or $\pi \rightarrow \sigma^*$) states gives rise to important one-center contribution to the coupling matrix element,[24b] and thus leading to out-of-plane contribution to the transition moment for singlet–triplet transitions. It was also recently suggested[25] that intermolecular charge-transfer interactions might lead to an out-of-plane contribution to the transition moments of singlet–triplet transitions in molecular aromatic crystals. However, as the oscillator strength for the singlet–singlet intermolecular charge-transfer optical transition is expected to be very low,[26] this intermolecular coupling mechanism will not lead to a substantial intensity borrowing for the triplet state. It is likely that the major contribution to the singlet–triplet transition moment out of the molecular plane arises from intramolecular spin–orbit coupling with $\pi\sigma^*$ (or $\sigma\pi^*$) singlet states.

VII. TRIPLET-EXCITON DIFFUSION COEFFICIENT IN THE ab PLANE

The diffusion coefficient of triplet excitons in crystalline anthracene was determined from the dependence of the emitted blue light intensity on the size of the illuminated circular or slab region. In these experiments, the incident light beam was kept perpendicular to the ab crystal plane. Typical experimental results are displayed in Figs. 6–8. For the case of the circular illuminated region, the experimental data were fitted to the results of machine calculations, while for the case of the slab region, Eq. (20) was employed for the interpretation of the experimental data. The analysis of the experimental results yields the values of $(D/\beta)^{\frac{1}{2}}$, i.e., the diffusion length. These results, combined with the triplet-exciton lifetimes, determined independently for each crystal, lead to the values of the exciton diffusion coefficients displayed in Table VII. The experimental values for the diffusion coefficients are independent of the shape of the irradiated area, yielding a strong support to the onalysis and interpretation of the experimental data. From these experiments we conclude that:

(a) The diffusion length varies from one crystal to another. A major part of these variations can be accounted for in terms of changes of the triplet-exciton lifetimes.

(b) The intensity of the blue light depends on the square of the incident light intensity (Fig. 8) over the whole range of R_0, in agreement with the results of the numerical calculations.

(c) The diffusion length is independent of the intensity and of the polarization direction of the exciting red light.

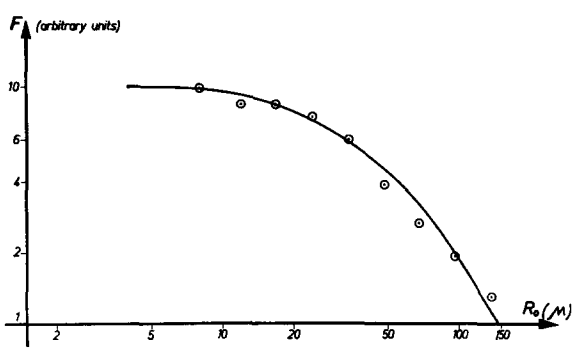

FIG. 6. The dependence of the intensity of the blue fluorescence for a circular irradiated area, on the radius R_0. Experimental data for a 0.4-mm zone-refined anthracene crystal irradiated perpendicular to the ab plane ($\beta = 180$ sec^{-1}). The calculated solid curve corresponds to $(D/\beta)^{\frac{1}{2}} = 10\ \mu$. F and R_0 are displayed on a logarithmic scale.

VIII. ANISOTROPY OF THE DIFFUSION TENSOR

The components of the diffusion tensor of triplet excitons in crystalline anthracene were determined by irradiating the crystal in a slab perpendicular to the a or b axes in the ab plane and to the a or c axes in the ac

TABLE VII. Diffusion coefficients for triplet excitons in the ab plane.

Crystal thickness (mm)	β (sec^{-1})	Spot shape	$(D/\beta)^{\frac{1}{2}}$ (μ)	$10^4 D$ (cm^2/sec)
0.5	200	Circle	8.5	1.4
0.4	180	Circle	10.0	1.8
0.4	180	Circle	9.5	1.6
0.4	180	Circle	9.7	1.7
0.5	180	Circle	11.0	2.1
0.4	200	Circle	10.0	2.0
0.4	180	Circle	12.0	2.5
0.5	200	Line	10.0	2.0
0.5	110	Line	15.0	2.3

[25] M. El-Sayed and N. K. Chadhuri, J. Chem. Phys. **43**, 1424 (1965).

[26] R. S. Berry, J. Jortner, J. C. Mackie, E. S. Pysh, and S. A. Rice, J. Chem. Phys. **42**, 1535 (1965).

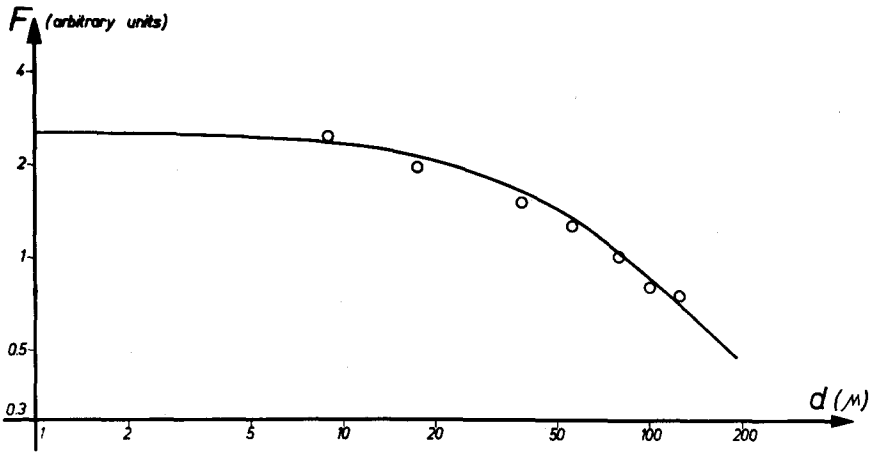

FIG. 7. The dependence of the intensity of blue fluorescence for an irradiated slab, on the effective thickness. Experimental data for a 0.3-mm zone-refined anthracene crystal irradiated perpendicular to the *ab* plane ($\beta=200$ sec^{-1}). Solid curve calculated for $(D/\beta)^{\frac{1}{2}}=10\ \mu$. F and d represented on a logarithmic scale.

plane. The experiments were performed on crystals characterized by the same triplet-exciton lifetimes ($\beta=115\pm10$ sec^{-1}). Experimental data were analyzed according to Eq. (20). In Fig. 9 we display the plots of Fd/C vs $1/d$. The values of $(\beta/D_{ii})^{\frac{1}{2}}$, which are proportional to the inverse of the diffusion length, could be estimated from the slope of the linear portion of the curve for large d values. The experimental results are displayed in Table VIII. These experimental data reveal no anisotropy of the triplet-exciton diffusion coefficient within a relatively large experimental error (or about 30%). The most surprising conclusion of this study is that the exciton diffusion tensor in crystalline anthracene is isotropic.

IX. DISCUSSION

In this work an attempt has been made to present experimental data for the diffusion triplet excitons in crystalline anthracene, in order to understand the mechanism of triplet-exciton dynamics in this system. The (isotropic) diffusion coefficient for triplet excitons $D=(2.0\pm0.5)\times10^{-4}$ cm^2/sec obtained herein is in excellent agreement with the data of Avakian and Merrifield.[11] The discrepancy between the results of the present work and the data of Kepler and Switendick[12] is rather disturbing, as the interpretation of the experimental data presented by these authors cannot be reconciled with the results of the present study. It should be noted that, in one of the experiments of Kepler and Switendick, triplet excitons are indirectly generated by a radiationless decay of singlet excitons. In these experiments, where ultraviolet light is absorbed at varying depths of the crystal, singlet exciton–exciton interactions[27] and surface ionization of singlet excitons, lead to charge-carrier production. An alternative channel for singlet–triplet conversion may involve singlet-exciton ionization, followed by subsequent electron–hole recombination leading to the formation

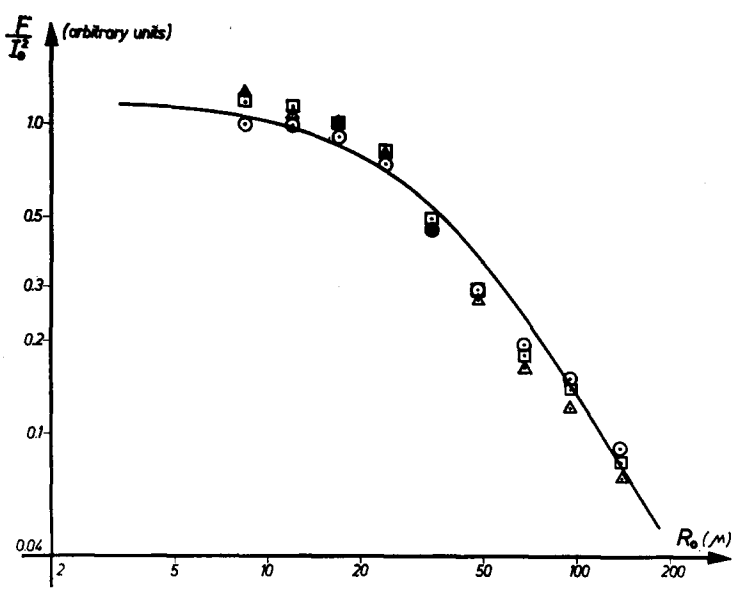

FIG. 8. The dependence of the total intensity of the blue fluorescence F on the total laser intensity I_0 (in arbitrary units). 0.4-mm-thick crystal ($\beta=200$ sec^{-1}) irradiated by a circular spot perpendicular to the *ab* plane. Solid curve calculated for $(D/\beta)^{\frac{1}{2}}=8.5\ \mu$. ⊙, $I_0=1$; ⊡, $I_0=0.5$; △, $I_0=0.25$.

[27] S. I. Choi and S. A. Rice, J. Chem. Phys. **38**, 366 (1964).

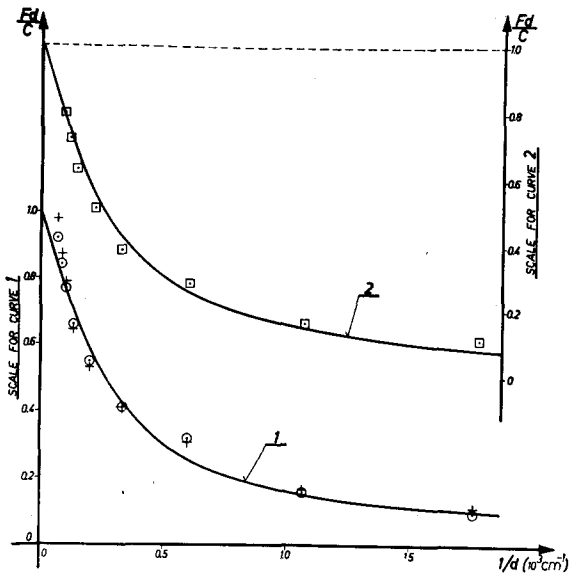

FIG. 9. The determination of the components of the diffusion tensor for triplet excitons in crystalline anthracene, for a 0.4-mm-thick zone-refined crystal with $\beta=115$ sec^{-1}. Curve 1: Crystal irradiated perpendicular to the ab plane; +, long axis of the slab parallel to the crystal b axis, the diffusion coefficient in the direction parallel to the a axis; O, long axis of the slab parallel to the crystal a axis, diffusion coefficient in the direction parallel to the b axis. Curve 2: Crystal irradiated perpendicular to the ac plane; □, long axis ot the slab parallel to the crystal a axis, the diffusion coefficient in the direction parallel to the c axis. The solid curves were calculated for $(D_{ii}/\beta)^{\frac{1}{2}}=15\ \mu$.

of triplet (or singlet) excitons. As the diffusion coefficient for electrons and holes in crystalline anthracene, estimated from the mobility data,[28] is of the order of 10^{-2} cm^2/sec, it is possible that in this experiment of Kepler and Switendick the diffusion coefficient of the charge carriers, rather than triplet-exciton diffusion, was determined.

The magnitude of the diffusion coefficient

$$[D(\text{exptl})=2\times10^{-4}\ \text{cm}^2/\text{sec}]$$

is in reasonable agreement with the theoretical results based on the hopping model $[D(\text{calc})=5\times10^{-4}$–$15\times10^{-4}$ cm^2/sec] and with the strong scattering limit of the band model $[D(\text{calc})=3\times10^{-4}$ cm^2/sec]. It is worthwhile again to point out that the numerical results of the theoretical analysis depend critically on the approximate molecular wavefunctions employed in the calculation of the intermolecular interactions and on the rough approximation used for the final density of states in the calculations of the transition probability. The theoretical calculations thus provide a reliable order of magnitude estimate of the diffusion coefficient. The comparison between the experimental and theoretical values for the diffusion coefficient presented herein yields evidence evidence for the validity of the strong scattering random-walk model for triplet-exciton migration in crystalline anthracene.

[28] R. Kepler, Phys. Rev. **119**, 1226 (1960).

Some kinetic implications of these results should now be considered. The experimental results for the diffusion coefficient yields a strong support for the proposal that in the case of triplet–triplet annihilation,[4] the rate-determining steps involve the production of two adjacent excited molecules, i.e., the bimolecular annihilation reaction is diffusion controlled.[13] The rate constant is then expected to be given by the rate for the encounter of two triplet excitons $\Gamma=8\pi D\langle R\rangle$ and a statistical factor $\eta=1/g$, representing the probability for the formation of a singlet state from a pair of triplet excitons, so that $\gamma=\eta\Gamma$, setting $\langle R\rangle=6$ Å, $D=2\times10^{-4}$ cm^2/sec we get $\gamma=2\times10^{-11}$ cm^3/sec, which is in excellent agreement with the experimental results[4,8,10] $[\gamma(\text{exptl})=2-6\times10^{-11}$ cm^3/sec]. These results imply that the mechanism recently proposed by Singh *et al.*[8] for the decomposition of a singlet exciton to give a pair of triplet excitons, which is just the reverse of the triplet–triplet annihilation reaction, is not amenable to experimental observation, as the recombination rate of triplet excitons is fast on the time scale of triplet-exciton migration.

The experimental data obtained for the anisotropy of the components of the diffusion tensor provide a critical check for the relative magnitude of the intermolecular pair interactions. It should be noted that on the basis of the relative magnitude of the components of the diffusion tensor one cannot distinguish between the band and the hopping models for triplet-exciton migration. The isotropy of the diffusion tensor in the ab plane $D_{aa}/D_{bb}(\text{exptl})=1.0\pm0.2$ is in excellent agreement with the theoretical results $D_{aa}/D_{bb}(\text{calc})=1.1$. It should be stressed, however, that while the experimental data for the diffusion coefficient in the ab plane are in good agreement with theory, the theoretical values for the diffusion coefficient of triplet excitons in the **c** direction are too small by about one to two orders of magnitude. The same difficulty is encountered in the theoretical study of the mobility of an excess electron in crystalline anthracene and naphthalene.[18,29] One can account for the experimental data by the conjecture

TABLE VIII. The anisotropy of the diffusion tensor for triplet excitons in crystalline anthracene ($\beta=110$ sec^{-1}, crystal thickness 0.4 mm).

Crystal direction i	$(D_{ii}/\beta)^{\frac{1}{2}}$ (μ) (exptl)	$(D_{ii}/\beta)^{\frac{1}{2}}$ (μ) (Calc)		
		Electron exchange (random walk)	Band model $\Lambda=5$ Å	Electron exchange +change transfer (random walk)
a	15	23	18	36
b	15	22	17	39
c	15	0.0	0.0	0.5

[29] J. L. Katz, S. I. Choi, S. A. Rice, and J. Jortner, J. Chem. Phys. **39**, 1683 (1963).

that phonons produce a large increase of the transfer integrals between molecules in two neighboring *ab* planes. This effect will enhance both the diffusion of triplet excitons and the excess electron mobility in this direction.

It would be interesting at this stage to relate the experimental results obtained for triplet-exciton dynamics with spectroscopic data. In the recent outstanding experiment of Hanson and Robinson,[15] the Davydov splitting in the first triplet state of crystalline naphthalene was directly determined. These experiments determine the intermolecular interaction between translationally inequivalent molecules $K[(\mathbf{a}+\mathbf{b})/2]=6$ cm^{-1} which is in good agreement with the theoretical result $K[(\mathbf{a}+\mathbf{b})/2]=7$ cm^{-1} calculated including electron exchange and charge-transfer interactions.[13,14] On the other hand, for the interaction between translationally equivalent molecules, the theory predicts $K(\mathbf{b})=5.6$ cm^{-1}, while from comparison of the energy of the emission line of $C_{10}H_8$ in $C_{10}D_8$ with the absorption line for the singlet–triplet transitions in pure $C_{10}H_8$, Hanson and Robinson conclude[15] that $K(\mathbf{b})\approx 0$ {i.e., $K(\mathbf{b})\ll K[(\mathbf{a}+\mathbf{b})/2]$}. Although it is somewhat speculative to extrapolate experimental (and theoretical) data from naphthalene to anthracene, the intermolecular interactions in these two crystals are very similar.[13,14,29] Assuming, for the case of anthracene, that $K(\mathbf{b})\ll K[(\mathbf{a}+\mathbf{b})/2]$ we get for the anisotropy of the diffusion tensor $D_{aa}/D_{bb}\approx 3$, in contradiction to the experimental results. We thus conclude that in the case of naphthalene it is also plausible that $K(\mathbf{b})\approx K[(\mathbf{a}+\mathbf{b})/2]$ in agreement with the results of the theoretical analysis. It thus appears that the contribution of intermolecular interaction between translationally equivalent molecules cannot be obtained from the experimental spectroscopic data of Hanson and Robinson,[15] as the environmental shifts for the system $C_{10}D_8/C_{10}H_8$ has to be treated using a general theory of shallow impurity states.[30]

ACKNOWLEDGMENTS

We are grateful to Professor S. A. Rice for helpful discussions. We wish to thank Dr. D. Kyser and Professor S. A. Rice for the generous supply of zone-refined anthracene crystals.

APPENDIX: AN ANALYTICAL SOLUTION OF THE DIFFUSION EQUATION

The solution of nonlinear differential equations is usually obtained by numerical integration using electronic computers. In this Appendix some analytical approximate methods are presented for the solution of the diffusion equation. They do not necessarily converge rapidly, but the general character of the solutions as well as their scaling properties can be inferred from them.

The particle current density for an isotropic diffusion is given by

$$\mathbf{j}=-D\,\mathrm{grad}\rho, \tag{A1}$$

where ρ is the particle density. In the nonisotropic case

$$j_\mu=\sum_\nu D_{\mu\nu}(\partial\rho/\partial X_\nu), \tag{A2}$$

where $\mu, \nu=1, 2, 3$ denote the rectangular coordinates x, y, z and D is a second-rank diffusion tensor.

The continuity equation has to be supplemented by source and sink terms which appear on the right-hand side

$$(\partial\rho/\partial t)+\mathrm{div}\mathbf{j}=-\beta\rho-\gamma\rho^2+S. \tag{A3}$$

Here β^{-1} is the lifetime of the exciton, γ is the bimolecular recombination rate constant, and the source term S describes the creation of the particles by the light. In the most general case, the bimolecular recombination rate constant depends on the direction, a term $-\rho\,\mathrm{div}\Gamma\,\mathrm{grad}\rho$ has to be added to the right-hand side of Eq. (A3), where Γ is a traceless second-rank tensor, describing the anisotropy of γ.

At first, the steady-state solution of the isotropic diffusion equation is sought for the case

$$0=D\nabla^2\rho-\alpha\rho-\gamma\rho^2+S. \tag{A4}$$

It is assumed that $\gamma\rho^2$ is a small term, and an iterative procedure will take it into account. This leaves the linear diffusion equation

$$0=D\nabla^2\rho-\alpha\rho+S, \tag{A5}$$

which separates in cylindrical coordinates. The eigenfunctions for a plane parallel slab are

$$\rho=\sum_{k,m}a_{km}\rho_{km},$$

$$\rho_{km}(r,\varphi,z)=R_{km}(r)\Phi_m(\varphi)Z_k(z),$$

$$\Phi_m(\varphi)=\cos[m(\varphi-\varphi_0)],$$

$$Z_k(z)=\cos k(z-z_0),$$

$$R_{km}(r)=b_1K_m(\kappa r)+b_2I_m(\kappa r),$$

$$\kappa=[(\alpha/D)-k^2]^{\frac{1}{2}}. \tag{A6}$$

Here K_m, I_m are hyperbolic Bessel functions as defined by Morse and Feshbach.[31] This general solution is useful for discussing surface diffusion and the ensuring boundary conditions. Our assumption is that the source is cylindrical, i.e., surface effects can be neglected.

The Green's function for this case ($k=0$) is that solution of

$$D\nabla^2\rho-\alpha\rho+\delta^{(2)}(\mathbf{r}-\mathbf{r}_0)=0 \tag{A7}$$

[30] G. F. Koster and J. C. Slater, Phys. Rev. **95**, 1167 (1954).

[31] P. M. Morse and H. Feshbach, *Methods of Mathematical Physics* (McGraw-Hill Book Co., Inc., New York, 1953).

which satisfies the boundary conditions.[32] It is $2K_0(\kappa R)$, where $\kappa=(\alpha/D)^{\frac{1}{2}}$, $R=|\mathbf{r}-\mathbf{r}_0|$. It can be expanded by an addition theorem

$$K_0(\kappa R)=\sum_{m=-\infty}^{\infty}\exp(im\varphi)\,J_m(\nu r)K_m(\kappa r_0), \qquad 0<r<r_0, \tag{A8}$$

$$=\sum_{m=-\infty}^{\infty}\exp(im\varphi)\,J_m(\kappa r_0)K_m(\kappa r), \qquad r>r_0>0.$$

Substitution into (A4) yields the integral equation

$$\rho(\mathbf{r})=\int_0^{2\pi}d\varphi_0\int_0^{\infty}r_0dr_0 2K_0(\kappa\mathbf{R})[S(\mathbf{r}_0)-\Gamma\rho^2(\mathbf{r}_0)], \tag{A9}$$

where $\Gamma=\gamma/D$. Also $K_0(\kappa\mathbf{R})$ can be expanded as in (A8). For a cylindrically symmetric source, the solution has to be symmetric too, thus only the term with $m=0$ has to be taken, and ρ is a function of $|\mathbf{r}|$ only:

$$\rho(r)=4\pi\Big\{K_0(\kappa r)\int_0^{r}I_0(\kappa r_0)[S(r_0)-\Gamma\rho^2(r_0)]r_0dr_0 +I_0(\kappa r)\int_r^{\infty}K_0(\kappa r_0)[S(r_0)-\Gamma\rho^2(r_0)]r_0dr_0\Big\}. \tag{A10}$$

The asymptotic behavior of the solutions can be investigated. If the source has finite size, the asymptotic behavior is governed by that of $K_0(\kappa r)$:

$$\rho(r)\sim r^{-\frac{1}{2}}\exp(-\kappa r).$$

This can be seen, noting that the integral multiplying $K_0(\kappa r)$ tends to a finite limit, and the second term is dominated by the first. The integral equation can be solved by an iteration procedure,

$$\rho_0(r)=0,$$

$$\rho_{n+1}(r)=4\pi\Big\{K_0(\kappa r)\int_0^{r}I_0(\kappa r_0)[S(r_0)-\Gamma\rho_n^2(r_0)]r_0dr_0 +I_0(\kappa r)\int_r^{\infty}K_0(\kappa r_0)[S(r_0)-\Gamma\rho_n^2(r_0)]r_0dr_0\Big\}, \tag{A11}$$

if $\rho_{n+1}(r)$ is positive; if it is negative, it has to be replaced by $\rho_{n+1}(r)=0$. This iteration procedure converges in principle, as it gives a series bounded by $\rho_1(r)$ from above, and by $\rho_2(r)$ from below. For small densities $\rho(r)\ll\Gamma^{-1}$, the iteration converges rapidly.

We next investigate a nontrivial problem, that of an elliptical source. First assume $\Gamma=0$:

$$S(r,\varphi)=S_0(r_0)+S_2(r_0)\cos2\varphi_0, \qquad 0\leq S_2(r_0)\leq S_0(r_0),$$

$$\rho(r,\varphi)=\rho_0(r)+\sum_{m=1}^{\infty}\rho_{2m}(r)\cos2m\varphi. \tag{A12}$$

The equation for $\rho_0(r)$ is just (A10) with $\Gamma=0$:

$$\rho_0(r)=4\pi\Big[K_0(\kappa r)\int_0^{r}I_0(\kappa r_0)S_0(r_0)r_0dr_0 +I_0(\kappa r)\int_r^{\infty}K_0(\kappa r_0)S_0(r_0)r_0dr_0\Big]. \tag{A13}$$

The equation for $\rho_2(r)$ is similar:

$$\rho_2(r)=2\pi\Big[K_2(\kappa r)\int_0^{r}I_2(\kappa r_0)S_2(r_0)r_0dr_0 +I_2(\kappa r)\int_r^{\infty}K_2(\kappa r_0)S_2(r_0)r_0dr_0\Big]. \tag{A14}$$

The more realistic case for $\Gamma\neq0$ can be expanded in a similar way, but the result is more complicated. From the above, the measured total blue light intensity can be calculated:

$$I_{\text{blue}}=2\pi\int[\rho_0^2(r)+\tfrac{1}{2}\rho_2^2(r)]rdr. \tag{A15}$$

Thus, in the region where $\Gamma^{-1}>\rho(r)$, i.e., the "quadratic" region, among all "red" sources of the same total intensity the one which gives the least "blue" intensity is the symmetric one. This theorem can be easily generalized. If the diffusion is not isotropic, i.e., Eq. (A2) can be written in its principal axes:

$$j_i=D_{ii}(\partial\rho/\partial X_i),$$
$$\operatorname{div}\mathbf{j}=\sum_i D_{ii}(\partial^2\rho/\partial X_i^2). \tag{A16}$$

In terms of the new coordinates,

$$\xi_i=(D_{ii})^{-\frac{1}{2}}X_i, \tag{A17}$$

the diffusion equation is isotropic. Therefore, in the "quadratic" region, if a "red" source of constant total intensity is made to vary in ellipticity, the ellipticity giving the smallest "blue" output corresponds to the ratio of the diffusion coefficients, according to the equation

$$d_i\sim(D_{ii})^{\frac{1}{2}}, \tag{A18}$$

where d_i denotes the size of the light source in the i direction. Similar considerations can be applied to the possible asymmetry of Γ.

[32] Here $\delta^{(2)}(\mathbf{r}-\mathbf{r}_0)$ denotes the two-dimensional delta function, $2\pi\int\delta^{(2)}(r)rdr=1$.